JOURNAL OF BACTERIOLOGY, June 2002, p. 3159–3166 Vol. 184, No. 12
0021-9193/02/$04.00+0 DOI: 10.1128/JB.184.12.3159–3166.2002

SitABCD Is the Alkaline Mn^{2+} Transporter of *Salmonella enterica* Serovar Typhimurium

David G. Kehres,[1]* Anuradha Janakiraman,[2] James M. Slauch,[2,3] and Michael E. Maguire[1]

Department of Pharmacology, School of Medicine, Case Western Reserve University, Cleveland, Ohio 44106-4965,[1] *and Department of Microbiology*[2] *and College of Medicine,*[3] *University of Illinois, Champaign, Illinois 61801*

Received 15 February 2002/Accepted 27 March 2002

MntH, a bacterial homolog of the mammalian natural resistance-associated macrophage protein 1 (Nramp1), is a primary Mn^{2+} transporter of *Salmonella enterica* serovar Typhimurium and *Escherichia coli*. *S. enterica* serovar Typhimurium MntH expression is important for full virulence; however, strains carrying an *mntH* deletion are only partially attenuated and display no obvious signs of Mn^{2+} deficiency. We noted that promoter sequences for *mntH* and for the putative Fe^{2+} transporter *sitABCD* appeared to have the same regulatory element responsive to Mn^{2+} and so hypothesized that *sitABCD* could transport Mn^{2+} with high affinity. We have now characterized transport by SitABCD in *S. enterica* serovar Typhimurium using $^{54}Mn^{2+}$ and $^{55}Fe^{2+}$ and compared its properties to those of MntH. SitABCD mediates the influx of Mn^{2+} with an apparent affinity (K_a) identical to that of MntH, 0.1 μM. It also transports Fe^{2+} but with a K_a 30 to 100 times lower, 3 to 10 μM. Inhibition of $^{54}Mn^{2+}$ transport by Fe^{2+} and of $^{55}Fe^{2+}$ transport by Mn^{2+} gave inhibition constants comparable to each cation's K_a for influx. Since micromolar concentrations of free Fe^{2+} are improbable in a biological system, we conclude that SitABCD functions physiologically as a Mn^{2+} transporter. The cation inhibition profiles of SitABCD and MntH are surprisingly similar for two structurally and energetically unrelated transporters, with a Cd^{2+} K_i of ≈1 μM and a Co^{2+} K_i of ≈20 μM and with Ni^{2+}, Cu^{2+}, and Fe^{3+} inhibiting both transporters only at concentrations of >0.1 mM. The one difference is that Zn^{2+} exhibits potent inhibition of SitABCD (K_i = 1 to 3 μM) but inhibits MntH weakly (K_i > 50 μM). We have previously shown that MntH transports Mn^{2+} most effectively under acidic conditions. In sharp contrast, SitABCD has almost no transport capacity at acid pHs and optimally transports Mn^{2+} at slightly alkaline pHs. Overall, coupled with evidence that each transporter is multiply but distinctly regulated at the transcriptional level, the distinct transport properties of MntH versus SitABCD suggest that each transporter may be specialized for Mn^{2+} uptake in different physiological environments.

MntH is a high-affinity Mn^{2+} transporter of *Salmonella enterica* serovar Typhimurium and *Escherichia coli* with good homology to the eukaryotic Nramp proteins, a family of proteins in the domains *Eucarya* and *Bacteria* (7), with putative homologs recently identified in some members of the domain *Archaea* (18). Nramp proteins are electrogenic divalent cation-proton transporters with broad specificity for transition metals. The best-characterized substrates for the mammalian systems are Mn^{2+} (14, 16) and Fe^{2+} (2, 11, 14, 21), although relative affinities and capacities for the various transition metal cations have not yet been published.

MntH mediates the influx of Mn^{2+} with an affinity of about 0.1 μM in *S. enterica* serovar Typhimurium and of 0.5 μM in *E. coli* (19). It can also transport Fe^{2+} but only with an affinity of >10 μM, far higher than physiological concentrations of free Fe^{2+}. Thus, we previously concluded that MntH functions physiologically as a primary Mn^{2+} influx system. This conclusion is consistent with functional data on Mn^{2+} uptake and related phenotypes in other species. Derepression of the *B. subtilis* MntH homolog increases sensitivity to growth inhibition by Mn^{2+} (25). A similar increase in Mn^{2+} sensitivity is seen in *E. coli* after overexpression of MntH (19). Some metal-dependent growth phenotypes are also affected by mutation of the *E. coli mntH* locus (24). Mn^{2+} inhibits Ni^{2+} uptake in *Xenopus* oocytes transfected with the *M. tuberculosis* MntH homolog Mramp (1). Collectively, these findings suggest that Mn^{2+} is of general importance in both free-living and pathogenic bacteria. This hypothesis is supported by the findings that MntH contributes to H_2O_2 resistance in both *E. coli* and *S. enterica* serovar Typhimurium, that *S. enterica* serovar Typhimurium *mntH* is induced upon entry into murine macrophages, and that *S. enterica* serovar Typhimurium MntH function is required for full virulence even in BALB/c mice which are themselves functionally Nramp1$^{-/-}$ (19).

Despite its apparent role as a primary Mn^{2+} influx system, *S. enterica* serovar Typhimurium and *E. coli* lacking *mntH* display no obvious growth deficiency attributable to Mn^{2+}, and as noted, virulence in mice is only partially attenuated. In contrast, lack of natural resistance-associated macrophage protein 1 (Nramp1) in the mouse has a clear phenotype of greatly increased sensitivity to a variety of pathogens (3, 5, 6, 12, 22, 23, 30). One possible explanation for the apparently less severe phenotype in *S. enterica* serovar Typhimurium is that the bacterium possesses another Mn^{2+} transport system that can partially or wholly suppress deficiencies due to loss of *mntH*. We had previously noted that the *S. enterica* serovar Typhimurium *mntH* promoter contains not only OxyR and Fur binding motifs but also a novel inverted repeat element. This putative *cis*-acting element is also present, intriguingly, in the promoter

* Corresponding author. Mailing address: Department of Pharmacology, School of Medicine, Case Western Reserve University, 10900 Euclid Ave., Cleveland, OH 44106-4965. Phone: (216) 368-6187. Fax: (216) 368-3395. E-mail: dgk2@po.cwru.edu.

of *sitABCD*, an ABC cassette-ATPase type transporter capable of Fe^{2+} transport (17, 31). The *sitABCD* locus resides on a pathogenicity island, and its mutation attenuates *S. enterica* serovar Typhimurium virulence. We hypothesized that SitABCD could transport Mn^{2+} with high affinity and that it might therefore serve as an alternative Mn^{2+} transporter under some physiological conditions. Our present data show that SitABCD is primarily a Mn^{2+} transporter rather than an Fe^{2+} transporter. Moreover, while the affinity of Mn^{2+} for each system is identical and independent of pH, their rates of uptake have quite different dependencies on pH, with SitABCD operating optimally at slightly alkaline pHs and MntH operating optimally at acid pHs, suggestive of distinct physiological roles.

MATERIALS AND METHODS

Bacterial strains. The *mntH sitABCD* double mutant strain MM2524 was constructed by P22 transduction of the *sitA100*::Mu*d*Cm allele from JS142 (also designated MM2495), which is ATCC 14028 *sitA100*::Mu*d*Cm (17), into MM2165, which is SL1344 *mntH11*::*kan* (19). The *sitA100*::Mu*d*Cm insertion is polar on the entire *sitABCD* operon (17). Strain MM2524 was transformed with pBluescript II SK+ (Stratagene, Inc.) to generate the *amp* but still doubly transporter-deficient strain MM2637. MM2524 was transformed with pDGK220 (19) to generate the *amp* and MntH-overexpressing strain MM2638 and with pAJ113 to generate the *amp* and SitABCD-overexpressing strain MM2639. pAJ113 is a derivative of pAJ107 (17) in which the insert has been reduced to the 4,697-bp *Bsg*I fragment extending from 290 bp 5′ of the *sitA* start codon to 975 bp 3′ of the *sitD* stop codon. MM2089 is wild-type *S. enterica* serovar Typhimurium SL1344. Since MM2638 and MM2639 require ampicillin in the growth medium (50 μg/ml) to maintain the overexpressing plasmids, we used MM2637 grown in the presence of ampicillin rather than MM2524 as our negative control for transport studies. For studies on wild-type cells, MM2089 and the negative-control MM2524 were grown in the absence of antibiotics.

Transport assay. Transport was performed as previously described (19) in intact cells carrying one or both of the MntH and SitABCD transporters. Manganese(II) uptake and iron(II) uptake were determined by incubating cells in DT medium (0.4% tryptone peptone, 0.25% NaCl) with $^{54}Mn^{2+}$ (Amersham) as used by Silver and colleagues (29), with duplicate or triplicate samples at each time point or concentration. Cells were then processed essentially as for Mg^{2+} transport assays from this laboratory (13). Cells were filtered with 0.45-μm-pore-size filters (BA85; Schleicher and Schuell), rinsed twice with 5 ml of ice-cold DT medium, and counted in BioSafe II scintillation cocktail (Research Products International, Inc.) in a Beckman LS6500 liquid scintillation counter. Channels 401 through 945 were used to detect photons derived from gamma radiation of $^{54}Mn^{2+}$. Beta radiation from $^{54}Mn^{2+}$, though more abundant, was also more variable due to inconsistent quenching in low-energy channels. $^{55}Fe^{2+}$ uptake was measured by detection of beta radiation in channels 1 through 400. Divalent cation solutions were made as 100 mM or 1 M stocks and diluted immediately before each assay. For Fe^{2+} and Fe^{3+}, fresh stocks were made immediately before the assay. The presence or absence of ascorbate had no effect on results in experiments with Fe^{2+}.

All data reported, except that in Fig. 7, are initial rates of transport. Transport via MntH was linear over time for at least 3 min, while transport via SitABCD was linear over time for at least 6 min at the cell and substrate concentrations required to achieve an amount of transport sufficient for statistical accuracy given the specific activity of the respective isotope. In experiments with wild-type cells, the respective maximal uptake capacities of the two transporters are proportional to their initial rates of uptake, since their apparent affinities for Mn^{2+} are identical (0.1 μM). Consequently, the absolute concentration of substrate cation is not a factor for such comparison. For the experiment with wild-type cells presented in Fig. 7, detection of $^{55}Fe^{2+}$ uptake required the use of a higher concentration of cells than in other experiments. Consequently, uptake of $^{54}Mn^{2+}$ measured under the identical conditions was linear for only 90 to 120 s rather than the somewhat longer times seen with lower cell numbers, thus dictating the choice of 1 min uptake values for comparison.

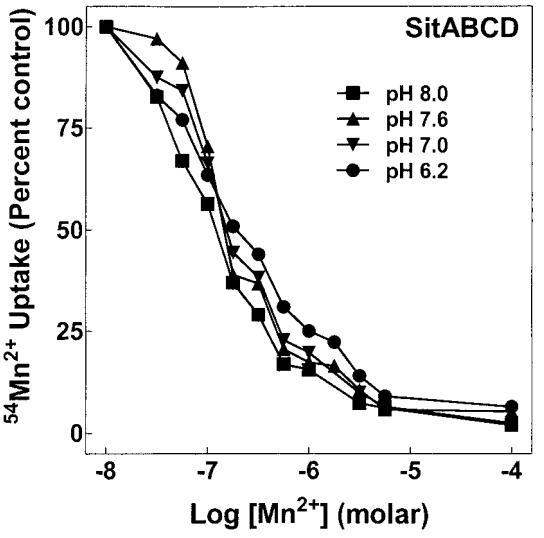

FIG. 1. Mn^{2+} affinity for SitABCD is below 1 μM and insensitive to pH. Mn^{2+} uptake by MM2639 (MM2524/pAJ113) was measured as described in Materials and Methods with 50 nM extracellular $^{54}Mn^{2+}$ and increasing concentrations of nonradioactive Mn^{2+} at the assay pH indicated, with each concentration tested twice. A single representative experiment of three similar experiments is shown. Errors ranged from about ±5% at low total Mn^{2+} concentrations to ±3% at higher Mn^{2+} concentrations.

RESULTS

SitABCD transport of Mn^{2+}. For measurement of transport, a stable insertion mutation in *sitABCD* and a stable deletion mutation in *mntH* were combined to create a strain with no detectable Mn^{2+} uptake (MM2524 [described in Materials and Methods]). Each system with its native promoter was added back individually on a relatively high-copy-number plasmid: pDGK220 in MM2524, generating MM2638 (for MntH) and pAJ113 in MM2524, generating MM2639 (for SitABCD). Overnight growth in M9 medium with glucose (M9/glucose medium) allowed sufficient expression for transport analysis. As illustrated in Fig. 1, MM2639 carrying only SitABCD transported $^{54}Mn^{2+}$ with an affinity of approximately 0.1 μM, identical to that for MntH. SitABCD affinity for Mn^{2+} was independent of pH, as for MntH (19).

Fe^{2+} inhibited Mn^{2+} uptake, but the K_i of Fe^{2+} inhibition for SitABCD was dependent on pH, ranging from about 50 μM at pH 8 to about 3 μM at pH 6.2 (Fig. 2). In contrast to ferrous iron, ferric iron inhibited Mn^{2+} uptake by SitABCD poorly, with a K_i of about 100 μM that was insensitive to pH. These properties of SitABCD interaction with iron were identical to those of MntH, except that the apparent K_i of SitABCD for Fe^{2+} was approximately 3- to 10-fold lower (better) than that of MntH for Fe^{2+}. SitABCD took up $^{55}Fe^{2+}$ (Fig. 3) with an apparent affinity and pH dependence that were completely consistent with the Fe^{2+} inhibition of Mn^{2+} transport (Fig. 2). Likewise, in the reverse experiment, the K_i for Mn^{2+} inhibition of $^{55}Fe^{2+}$ uptake was insensitive to pH and equal to the apparent affinity (K_a) for $^{54}Mn^{2+}$ uptake (data not shown). The salient result is that the affinity for Mn^{2+} is 10 to 100 times better than that for Fe^{2+} for both transporters, regardless of

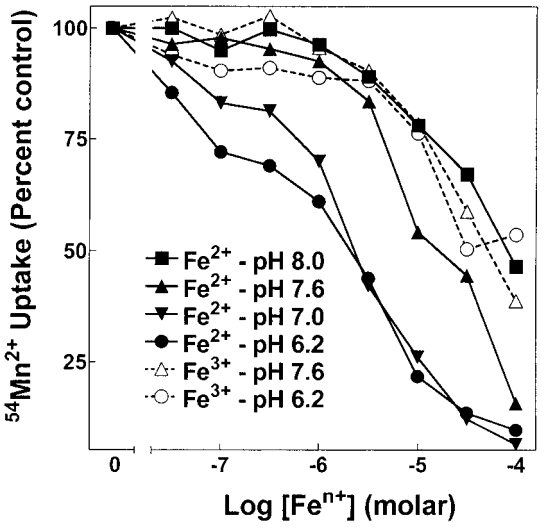

FIG. 2. Fe^{2+} but not Fe^{3+} inhibition of SitABCD Mn^{2+} uptake is sensitive to pH. Mn^{2+} uptake by MM2639 (MM2524/pAJ113) was measured as described in Materials and Methods with 50 nM extracellular $^{54}Mn^{2+}$ and increasing concentrations of nonradioactive Fe^{2+} or Fe^{3+} at the assay pH indicated, with each concentration tested twice. Assays with Fe^{2+} contained 1 mM ascorbate. A control experiment showed that ascorbate did not affect transport by SitABCD. One of two similar experiments is shown. Errors ranged from about ±4% at low total Mn^{2+} concentrations to ±2% at higher Mn^{2+} concentrations.

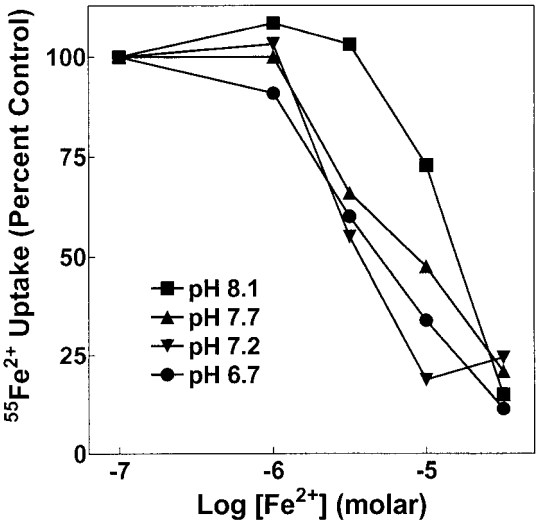

FIG. 3. Fe^{2+} affinity for SitABCD is greater than 1 μM and sensitive to pH. $^{55}Fe^{2+}$ uptake by SitABCD was measured in MM2639 (MM2524/pAJ113) as described in Materials and Methods with 100 nM extracellular $^{55}Fe^{2+}$ and increasing concentrations of nonradioactive Fe^{2+} at the assay pH indicated, with each concentration tested twice. A single representative experiment of three similar experiments is shown. Errors ranged from about ±5% at low total Fe^{2+} concentrations to ±3% at higher Fe^{2+} concentrations.

pH sensitivity. Further, SitABCD could not mediate uptake of $^{55}Fe^{3+}$ (data not shown). Since micromolar concentrations of free iron are generally not found in biological systems, SitABCD, like MntH, appears to function primarily as a Mn^{2+} influx system.

Cation selectivity of SitABCD transport. Inhibition of SitABCD-mediated Mn^{2+} uptake by various transition metal cations paralleled their inhibition of MntH, with Cd^{2+} being the most potent (K_i = 1 to 3 μM). Co^{2+} inhibited uptake with a K_i of about 20 μM, while Cu^{2+}, Ni^{2+}, and Fe^{3+} inhibited uptake with K_is of >100 μM (Fig. 4A). The major difference between SitABCD and MntH was that Zn^{2+} inhibited SitABCD with an affinity of 1 to 3 μM that was not significantly sensitive to pH (Fig. 4B). In contrast, the MntH affinity for Zn^{2+} (19), also pH insensitive, was about 50 times poorer than that of SitABCD for Zn^{2+}. Further, the K_i of Zn^{2+} for inhibition of $^{54}Mn^{2+}$ uptake via SitABCD was identical to its K_i for inhibition of $^{55}Fe^{2+}$ uptake by SitABCD (data not shown). Thus, the interactions of the various cations with both SitABCD (this report) and MntH (19) are consistent with competitive inhibition.

pH dependence of SitABCD transport. The V_{max} of MntH for Mn^{2+} uptake increases as pH decreases (19). We therefore determined the pH profile for SitABCD uptake of Mn^{2+}. In contrast to the acid pH optimum of MntH, SitABCD displayed a very marked increase in transport rate with increasing alkalinity (Fig. 5). While MntH can take up substantial amounts of Mn^{2+} at both acid and slightly alkaline pHs, SitABCD was almost inactive at acid pHs, with uptake rising to significant levels near neutrality and remaining essentially constant thereafter. Since the transport capacities (V_{max}) of MntH and SitABCD appeared comparable (Fig. 6), these data suggested that under routine growth conditions, overall Mn^{2+} accumulation by wild-type cells expressing both transporters would be due predominantly to SitABCD at alkaline pHs and due almost completely to MntH at acid pHs. The ability of Zn^{2+} to differentially inhibit the two systems provided the means to test this hypothesis.

Wild-type *S. enterica* serovar Typhimurium was grown overnight in M9/glucose medium; $^{54}Mn^{2+}$ uptake was then measured in morpholineethanesulfonic acid (MES)-HEPES-buffered transport medium at different pHs with and without addition of 20 μM Zn^{2+}, a concentration that inhibits 85 to 90% transport by SitABCD but less than 15% of that by MntH at each pH assayed. Since Mn^{2+} has equal affinities for these transporters and because the transporters are being expressed from their normal chromosomal background, the activity of each transporter relative to the other can be directly compared. Decomposition of total transport into MntH versus SitABCD contributions based on Zn^{2+} inhibition (Fig. 6A) demonstrated that both transporters were active simultaneously in wild-type cells. Furthermore, the inferred pH profiles of each transporter (Fig. 6A) were equivalent to those obtained in strains expressing only MntH or only SitABCD from plasmids (Fig. 5), thus validating the Zn^{2+} inhibition method. The results confirmed the hypothesis that at acid pHs, virtually all Mn^{2+} uptake is due to MntH. In contrast, while uptake by SitABCD was the major factor at alkaline pHs, MntH also contributed a significant amount of Mn^{2+} uptake.

Since the V_{max} of uptake by each system was dependent on pH, we asked if wild-type cells might respond to changes in the pH of the growth medium by adjusting the ratio of MntH to SitABCD activity that they express. Therefore, wild-type *S. enterica* serovar Typhimurium was subjected to growth at dif-

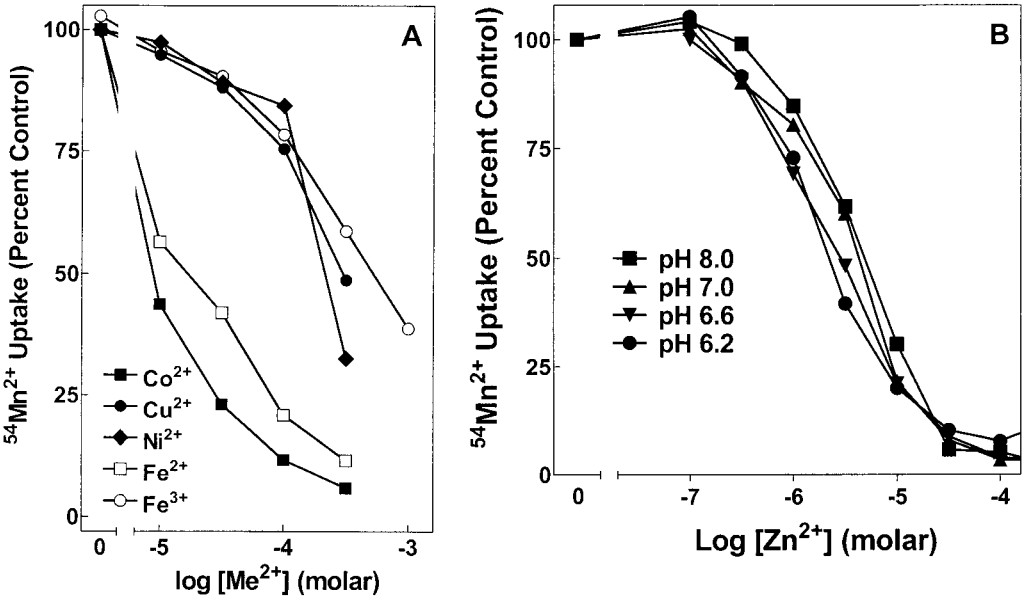

FIG. 4. Inhibition of Mn^{2+} uptake through SitABCD by other transition metal cations. Mn^{2+} transport by MM2639 (MM2524/pAJ113) was measured as described in Materials and Methods with 50 nM extracellular $^{54}Mn^{2+}$ and increasing concentrations of inhibitory cation at pH 7.2 (A) or increasing concentrations of Zn^{2+} at the indicated pH (B). One of two similar experiments is shown. Ascorbate at 1 mM was present in experiments with Fe^{2+}. Errors ranged from about ±5% at low total cation concentrations to ±3% at higher cation concentrations.

ferent pHs overnight. Then each culture was assayed for $^{54}Mn^{2+}$ uptake over the same range of pHs in the presence and absence of 20 μM Zn^{2+} as in Fig. 6A. The data indicated that while the absolute amount of Mn^{2+} uptake did increase slightly with increasing growth pH, the relative contributions of SitABCD and MntH to total Mn^{2+} uptake did not (Fig. 6B).

Physiological relevance of SitABCD transport of Mn^{2+}. The affinities of both SitABCD and MntH for Mn^{2+} are much higher than those for Fe^{2+}. This fact, coupled with the fact that the concentrations of free iron in biological systems are extremely low, argues that both transporters function as primary Mn^{2+} influx systems and that their ability to transport Fe^{2+} is of little physiological consequence. However, this supposition depends on the actual activity of each system in the cell in the context of overall homeostatic mechanisms operative for Mn^{2+} versus Fe^{2+}. To test the hypothesis that MntH and SitABCD are important to overall Mn^{2+} but not Fe^{2+} balance, we grew cells overnight in M9/glucose medium and measured both initial uptake rate and the equilibrium accumulation of Mn^{2+} and Fe^{2+}, comparing the behavior of a wild-type strain (MM2089) to that of a strain lacking both transporters (MM2524). We tested uptake at two concentrations, 50 nM and 1 μM. The lower concentration is about 30% of the apparent K_a of both transporters for Mn^{2+}, while 1 μM is about 10 to 30% of the apparent K_a of each transporter for Fe^{2+}. At room temperature, wild-type cells took up 50 nM Mn^{2+} with an initial rate of ≈50 pmol min^{-1} 10^9 $cells^{-1}$, reaching equilibrium in 30 min with a total Mn^{2+} uptake of about 100 pmol of Mn^{2+} per 10^9 cells (Fig. 7). This is equivalent to a total internal Mn^{2+} concentration of 100 μM, assuming a cytoplasmic volume of 1 μm^3 per cell (19). By contrast, in the strain lacking both transporters, there was no significant Mn^{2+} uptake over the first 15 min, and after 30 min, only about 2 pmol of Mn^{2+} per 10^9 cells had been accumulated. Even at 1 μM external Mn^{2+}, the transporter-deficient strain accumulated only 20 pmol of Mn^{2+} per 10^9 cells after 30 min compared to about 300 pmol per 10^9 cells for the wild-type strain. This residual uptake in the double knockout strain was presumably either through an additional low-capacity Mn^{2+}-selective transporter or by leakage through a transporter for another cation.

Lack of physiological relevance of Fe^{2+} uptake by SitABCD. In contrast to the extensive Mn^{2+} uptake in wild-type cells, there was no detectable uptake of 50 nM extracellular Fe^{2+} after 30 min of incubation in either strain (data not shown). When Fe^{2+} was supplied at 1 μM, a concentration more commensurate with the K_as of the transporters for this cation, the initial rate of uptake by wild-type cells was >30 pmol of Fe^{2+} min^{-1} 10^9 $cells^{-1}$, while the double knockout strain took up about 10 pmol of Fe^{2+} min^{-1} 10^9 $cells^{-1}$. This difference between the initial uptake rate of the wild-type and double knockout strains was qualitatively reproducible but quite variable from experiment to experiment, the difference ranging from 5 to 20 pmol of Fe^{2+} min^{-1} 10^9 $cells^{-1}$. This may reflect a variable background of externally bound iron not removed by washing at this relatively high Fe^{2+} concentration. At equilibrium after 30 min, total accumulation from medium with 1 μM Fe^{2+} reached ≈170 pmol of Fe^{2+} per 10^9 cells in the wild-type strain and ≈160 pmol of Fe^{2+} per 10^9 cells in the strain lacking both MntH and SitABCD (Fig. 7). This Fe^{2+} uptake in each strain was presumably through the divalent ferrous ion transporter FeoB (15) or, less likely, through siderophore-mediated Fe^{3+} systems in the event that a significant amount of Fe^{2+} was oxidized to the ferric form despite the presence of 1 mM ascorbate. Similar experiments at different pHs, lower cell concentrations, or cation concentrations 5- to 10-fold above the respective K_as gave similar results (data not shown). Thus,

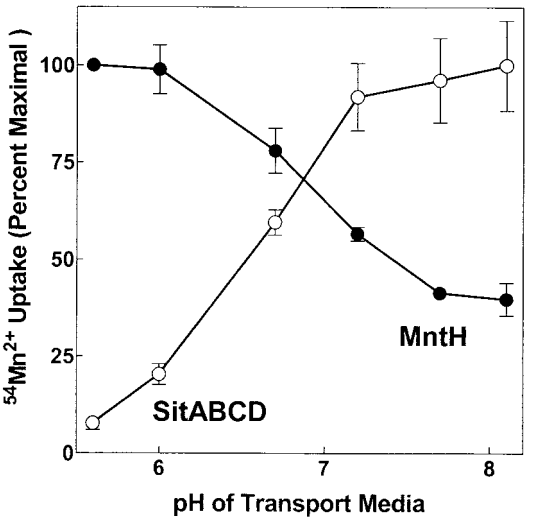

FIG. 5. The V_{max}s of MntH and SitABCD have an opposite pH dependence. Initial rates of 50 nM $^{54}Mn^{2+}$ uptake were measured as described in Materials and Methods for each individual transporter. MntH uptake was measured using MM2638 (MM2524/pDGK220), and SitABCD uptake was measured using MM2639 (MM2524/pAJ113). The absolute transporter activities of MntH and SitABCD differed slightly, because pDGK220 is a higher-copy-number plasmid than pAJ113 and because the promoters for each transporter likely respond somewhat differently to overnight growth in M9/glucose medium. Consequently, uptake by each transporter was normalized to the maximal uptake obtained, pH 5.5 for MntH and pH 8.2 for SitABCD. Within each strain however, the changes in initial rate with the assay pH of the transport medium accurately reflect the pH dependence of that transporter's V_{max}.

under these growth conditions, MntH and SitABCD combine to supply essentially all of the cell's Mn^{2+} but make no significant contribution to Fe^{2+} uptake or homeostasis.

DISCUSSION

Mechanistic properties of MntH and SitABCD transport. The transport properties of SitABCD (this report) and MntH (19), as measured in intact cells, are surprisingly similar for transporters with completely different structures and modes of energy coupling. Their apparent capacities (V_{max}) are comparable (Fig. 6), subject only to the caveat that the copy number of each transporter in the membrane is unknown. Their K_a or K_i values for Mn^{2+}, Co^{2+}, Ni^{2+}, Cu^{2+}, Cd^{2+}, and Fe^{3+} are virtually identical. SitABCD has a slightly lower (better) affinity for Fe^{2+} than does MntH. The affinity of each transporter for Mn^{2+} is completely unaffected by large changes in the pH. Likewise, both transporters exhibit a curious pH-dependent increase in affinity for Fe^{2+} and all inhibitory transition metal cations tested, except Zn^{2+} and Fe^{3+}.

The only transport properties in which the two systems differ are their relative sensitivity to Zn^{2+} inhibition and the pH dependence of their transport capacity. Zn^{2+} is a good inhibitor of SitABCD but has a much poorer K_i for MntH. This difference is probably of inconsequential significance physiologically. However, since MntH and SitABCD appear to be the only Mn^{2+} transporters of *S. enterica* serovar Typhimurium (Fig. 7), this difference has the practical consequence that we can obtain a measure of the relative contributions of SitABCD versus MntH for Mn^{2+} uptake by determining the Zn^{2+}-inhibitable versus Zn^{2+}-uninhibitable fraction of total Mn^{2+} (Fig. 5 and 6). The opposite trend in pH dependence of V_{max} for SitABCD and MntH transport has physiological implications (discussed below).

The finding that the K_a of Mn^{2+} uptake is independent of pH while that for Fe^{2+} is quite sensitive to pH likely has significant mechanistic implications for both transporters. With MntH, computer topology predictions indicate the presence of 11 transmembrane segments, one fewer than for homologous eukaryotic transporters. Clusters of histidine residues are also predicted at the cytosolic end of transmembrane domain 6 and periplasmic end of transmembrane domain 7. The pK_a of histidine is 6.5 and so is titrable over the pH range tested for transport. Histidines readily bind divalent cations and therefore are good candidates to mediate pH sensitivity of a protein. For example, Gerchman et al. (10) and Rimon et al. (26) have demonstrated that an intramembrane histidine controls much of the pH sensitivity of the NhaA Na^+/H^+ antiporter of *E. coli*. However, it seems unlikely that the histidines clustered around transmembrane domains 6 and 7 of MntH are involved in rate-limiting Mn^{2+} transport steps, since the K_a for Mn^{2+} uptake is insensitive to pH. Their involvement in Fe^{2+} transport by MntH is also problematic, given that the apparent K_a of MntH for Fe^{2+} decreases with increasing acidity. Since decreasing pH should protonate histidine, it seems unlikely that interaction of a positively charged cation with a protonated histidine near or within the transport channel would result in an increased cation affinity. Structural predictions for a multisubunit ABC type transporter like SitABCD are less straightforward than for a single polypeptide transporter. However, it is likewise equally problematic to attribute the different pH responses of SitABCD Mn^{2+} and Fe^{2+} affinities to histidine protonation or deprotonation. The pH dependence of the V_{max} for SitABCD, by contrast, is consistent with titration of a histidine. Protonation of one or more histidines at acidic pHs might well inhibit passage of a cationic substrate at a transport step well after the binding events that determine apparent K_a.

How then might these transporters have a Mn^{2+} affinity that is not sensitive to pH, yet a Fe^{2+} transport affinity (and inhibitory affinity for many other cations) that is sensitive to pH? There are two kinetic explanations. First, the K_a could be dominated by the association and dissociation rates of the substrate coupled with binding of Mn^{2+} to a qualitatively different site on the transporter than that for Fe^{2+} and the pH-sensitive inhibitory cations. Second, K_a could be influenced by the forward rate of transport coupled with the passage of Mn^{2+} through each transporter involving interactions not experienced by other cations. Although these explanations cannot be tested without a detailed structural analysis, we favor the first explanation. Ferric iron, Fe^{3+}, which is not transported, inhibits Mn^{2+} transport with a K_i as insensitive to pH as is the K_a for Mn^{2+} transport. Inhibition without transport implies binding without significant penetration of the membrane, i.e., Fe^{3+} binds to the periplasmic face of MntH and either remains sequestered in the periplasmic binding protein SitA or binds to the periplasmic face of the SitC and/or SitD membrane-spanning permease subunits. Thus, we would pre-

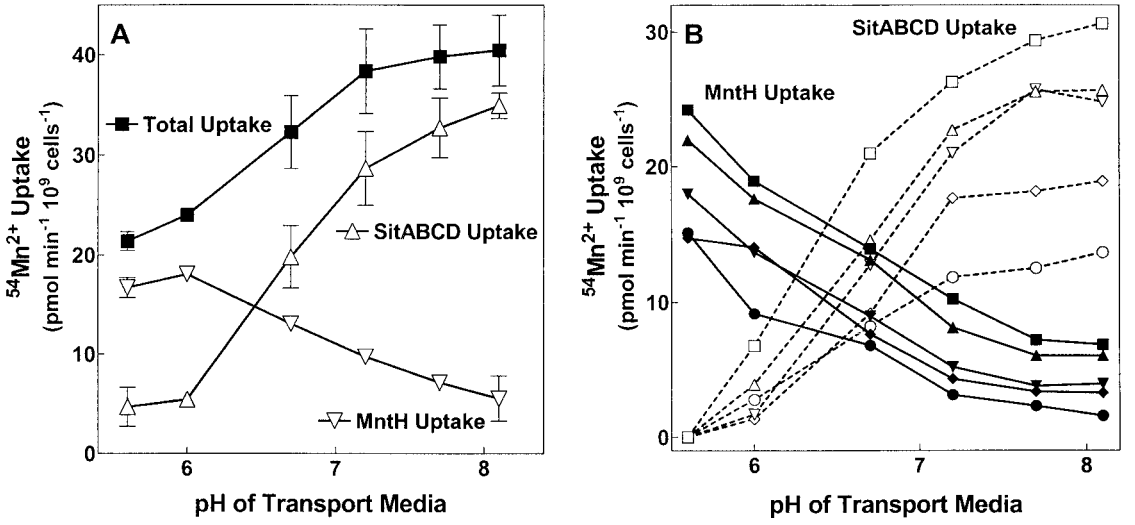

FIG. 6. Discriminating between MntH- and SitABCD-mediated Mn^{2+} uptake in wild-type cells. (A) MntH and SitABCD have comparable overall activities in cells grown in M9/glucose medium. Standard curves (not shown) had previously determined the percent resistance of MntH alone and SitABCD alone to 20 μM Zn^{2+} at a variety of assay pHs, using strains MM2638 and MM2639, respectively. At this Zn^{2+} concentration, MntH was always more than 85% resistant and SitABCD was always less than 15% resistant. In the experiment shown, wild-type *S. enterica* serovar Typhimurium (MM2089) was grown overnight in M9/glucose medium (pH 7.2), and uptake of 50 nM $^{54}Mn^{2+}$ was measured at different transport pHs with and without 20 μM Zn^{2+}. Total uptake was decomposed into MntH versus SitABCD components by linear interpolation of the measured Zn^{2+}-resistant uptake (not shown) using the standard curves previously generated with each point determined in duplicate. One of two similar experiments is shown. Unlike the experiment in Fig. 5, where the transporters are expressed from plasmids, in this experiment both transporters are being expressed in their normal chromosomal background. Since each transporter has the same affinity for Mn^{2+}, the initial rates of uptake are an accurate reflection of relative activity of each system. (B) Relative MntH and SitABCD activity does not vary with growth pH. Experiments equivalent to those shown in panel A were performed on wild-type cells (MM2089) grown in medium identical to M9/glucose medium except that the proportions of Na_2HPO_4 and KH_2PO_4 were varied to achieve different final growth pHs of 8.0 (■, □), 7.6 (▲, △), 7.2 (▼, ▽), 6.8 (◆, ◇), and 6.4 (●, ○) and assayed at the pH indicated on the *x* axis. SitABCD (open symbols) versus MntH (closed symbols) components of total uptake were calculated as in panel A. Total uptake curves have been omitted for clarity, but their shapes are similar to that shown in panel A. One of two similar experiments is shown. Errors ranged from about ±5% at low total Mn^{2+} concentrations to ±3% at higher Mn^{2+} concentrations.

dict that for each transporter, Mn^{2+} and Fe^{3+} would occupy the same binding pocket primarily responsible for determining affinity, while Fe^{2+} and the pH-dependent inhibitory cations either bind at a different site or bind with qualitatively different energetics at the same site.

The chemistry of these transition metal cations supports this interpretation. Of all the cations tested, only Fe^{3+} is isoelectronic with Mn^{2+}, having the spherically symmetric high-spin d^5 electron configuration often associated with labile binding due to weak *d* orbital coupling with biological ligands (8), thus allowing Fe^{3+} to coordinate similarly to Mn^{2+}. In contrast to Mn^{2+} and Fe^{3+}, Fe^{2+} (d^6) and most other inhibitory transition metal divalent cations interact with the protein via nonequivalent *d* orbitals. Metals with nonequivalent *d* orbital configurations bind with qualitatively different energetics to biological ligands (8). Supporting this interpretation is the result that Zn^{2+}, which also has a spherically symmetrical (d^{10}) electron configuration, also inhibits both transporters without pH dependence (Fig. 4B). Overall, these considerations suggest that for both transporters, both the K_is of inhibitory and K_as of substrate metals are determined by their association and dissociation rates rather than subsequent transport steps. Further, these rates appear to be influenced more by the *d* orbital configuration than by the charge of the interacting cation.

In addition to these chemical considerations, it is possible that the pH sensitivity of MntH and SitABCD is also related to the stoichiometry of transport. The mammalian NRAMP2 transporter was shown initially to be a H^+/cation symporter and is thus highly electrogenic (14). More recent data have confirmed this interpretation but also suggested that some NRAMP class transporters can mediate antiport of proton and divalent cations (11) and that the symport pathway has a variable stoichiometry for H^+, with more than one proton being transported per divalent cation transported (27). Symport or antiport of other ions would be unusual for SitABCD as a member of the ABC cassette superfamily; however, the relative stoichiometry of substrate translocation and ATP hydrolysis has not been determined and could conceivably be variable. Overall, the electrophysiological data for eukaryotic MntH homologs (11, 14, 27) and our demonstration of different pH-sensitive proton-cation interactions for different cations with both MntH and SitABCD promises complex but highly interesting mechanisms of transport.

Physiological implications. The finding that SitABCD and MntH have complementary pH profiles for their transport capacity offers an obvious rationale for why *S. enterica* serovar Typhimurium has two Mn^{2+} transporters. In the moderately acid environment that bacteria encounter in the mammalian small intestine or inside a developing phagosome, MntH would appear to offer the only means for significant Mn^{2+} uptake. In a moderately alkaline environment, by contrast, both MntH and SitABCD would have significant activity, thus affording the cell the luxury of coupling Mn^{2+} uptake either to the transmembrane proton gradient or to ATP hydrolysis according to

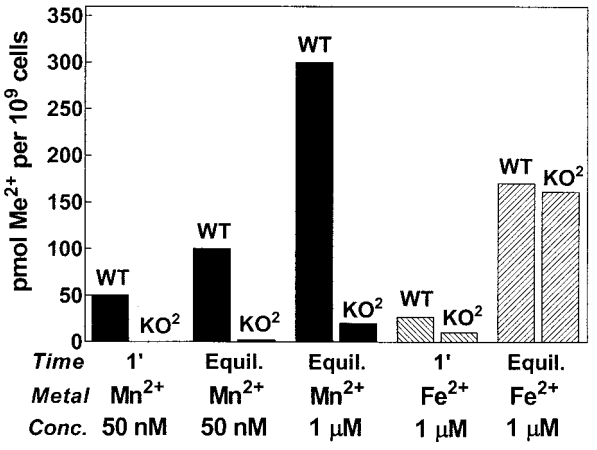

FIG. 7. SitABCD and MntH are responsible for physiological Mn^{2+} uptake but not Fe^{2+} uptake. Initial rates of uptake (1 min [1′]) of $^{54}Mn^{2+}$ at 50 nM (solid bars) and of $^{55}Fe^{2+}$ at 1 μM (hatched bars) are shown along with accumulation at equilibrium (30 min) for $^{54}Mn^{2+}$ at 50 nM or 1 μM (solid bars) or for $^{55}Fe^{2+}$ at 1 μM (hatched bars). Uptake by wild-type cells (MM2089) (WT) and by the *mntH sitABCD* double mutant strain (MM2524) (KO^2) is indicated. Concentrations of 50 nM Mn^{2+} and 1 μM Fe^{2+} were chosen for comparison, since these concentrations are essentially equivalent with respect to that cation's apparent K_a, thus allowing direct comparison of bulk uptake. Errors were about ±4% for Mn^{2+} and ±6% for Fe^{2+} uptake except for uptake of $^{55}Fe^{2+}$ at 1 min (see text). Equil., equilibrium.

its energetic capabilities and needs. The few MntH orthologs characterized thus far all transport more robustly at acid pHs than at alkaline pHs. Whether ABC-type Mn^{2+} transporters in other species such as YfeABCD (4) in the closely related *Yersinia pestis* (which also has an MntH) have the same alkaline pH dependence for their V_{max} as SitABCD is not yet known.

Whether MntH and SitABCD are expressed more asymmetrically in environments other than the high-phosphate minimal M9/glucose medium is not known. It may be that the current and anticipated Mn^{2+} requirements of cells comfortably supplied with glucose are so slight that both transporters are only minimally expressed, regardless of growth pH. More likely, the minimal transition metal content of M9/glucose medium leads to maximal expression of both transporters, regardless of growth pH.

Whether MntH and SitABCD are relevant to Fe^{2+} uptake and iron homeostasis in any other environments is not known, but in M9/glucose medium, Fe^{2+} uptake by these transporters is physiologically irrelevant. As shown in Fig. 7, when Fe^{2+} is supplied at 1 μM, roughly 20% of each transporter's K_a for Fe^{2+}, the wild-type strain internalizes at most 5 to 10% more iron than the *mntH sitABCD* double mutant. Since a free Fe^{2+} concentration of 1 μM or higher is very improbable, the contribution of MntH and SitABCD to iron homeostasis in any foreseeable *S. enterica* serovar Typhimurium environment will be far lower. By contrast, when Mn^{2+} is supplied at roughly 30% of each transporter's K_a for Mn^{2+}, wild-type *S. enterica* serovar Typhimurium internalizes 40% of the total extracellular Mn^{2+} available compared to less than 1% in the *mntH sitABCD* double mutant. Thus, in standard media for enterobacteria, both MntH and SitABCD are functionally completely specific for Mn^{2+}. We note that, in contrast to the improbability of micromolar concentrations of free iron, a concentration of 50 to 100 nM Mn^{2+} is similar to estimated Mn^{2+} concentrations in plasma in mammals (9, 20, 28).

Overall, our demonstration that SitABCD transports Mn^{2+} in a physiologically relevant manner, coupled with the differences in pH dependence between *mntH* and *sitABCD* and the complex regulation of both transporters (19, 19a) leads to the conclusion that overall Mn^{2+} homeostasis is of some importance to the cell. Why Mn^{2+} homeostasis is of importance presumably resides in the functions of the relatively few known Mn^{2+} enzymes, an area of little knowledge but great potential.

ACKNOWLEDGMENTS

We thank James Cowan for many fruitful discussions of bioinorganic chemistry.

This work was supported in part by NIH grant GM61748 to M.E.M. and grant 00-25 from the Roy J. Carver Charitable Trust to J.M.S.

REFERENCES

1. **Agranoff, D., I. M. Monahan, J. A. Mangan, P. D. Butcher, and S. Krishna.** 1999. *Mycobacterium tuberculosis* expresses a novel pH-dependent divalent cation transporter belonging to the Nramp family. J. Exp. Med. **190:**717–724.
2. **Atkinson, P. G., and C. H. Barton.** 1998. Ectopic expression of Nramp1 in COS-1 cells modulates iron accumulation. FEBS Lett. **425:**239–242.
3. **Barton, C. H., S. H. Whitehead, and J. M. Blackwell.** 1995. Nramp transfection transfers Ity/Lsh/Bcg-related pleiotropic effects on macrophage activation: influence on oxidative burst and nitric oxide pathways. Mol. Med. **1:**267–279.
4. **Bearden, S. W., and R. D. Perry.** 1999. The Yfe system of *Yersinia pestis* transports iron and manganese and is required for full virulence of plague. Mol. Microbiol. **32:**403–414.
5. **Bellamy, R., and A. V. Hill.** 1998. Genetic susceptibility to mycobacteria and other infectious pathogens in humans. Curr. Opin. Immunol. **10:**483–487.
6. **Cellier, M., G. Govoni, S. Vidal, T. Kwan, N. Groulx, J. Liu, F. Sanchez, E. Skamene, E. Schurr, and P. Gros.** 1994. Human natural resistance-associated macrophage protein: cDNA cloning, chromosomal mapping, genomic organization, and tissue-specific expression. J. Exp. Med. **180:**1741–1752.
7. **Cellier, M. F., I. Bergevin, E. Boyer, and E. Richer.** 2001. Polyphyletic origins of bacterial Nramp transporters. Trends Genet. **17:**365–370.
8. **Cowan, J. A.** 1997. Inorganic biochemistry: an introduction, p. 1–63. Wiley-VCH, New York, N.Y.
9. **Galeotti, T., G. Palombini, and G. D. van Rossum.** 1995. Manganese content and high-affinity transport in liver and hepatoma. Arch. Biochem. Biophys. **322:**453–459.
10. **Gerchman, Y., Y. Olami, A. Rimon, D. Taglicht, S. Schuldiner, and E. Padan.** 1993. Histidine-226 is part of the pH sensor of NhaA, a Na^+/H^+ antiporter in *Escherichia coli*. Proc. Natl. Acad. Sci. USA **90:**1212–1216.
11. **Goswami, T., A. Bhattacharjee, P. Babal, S. Searle, E. Moore, M. Li, and J. M. Blackwell.** 2001. Natural-resistance-associated macrophage protein 1 is an H^+/bivalent cation antiporter. Biochem. J. **354:**511–519.
12. **Govoni, G., and P. Gros.** 1998. Macrophage NRAMP1 and its role in resistance to microbial infections. Inflamm. Res. **47:**277–284.
13. **Grubbs, R. D., M. D. Snavely, S. P. Hmiel, and M. E. Maguire.** 1989. Magnesium transport in eukaryotic and prokaryotic cells using magnesium-28 ion. Methods Enzymol. **173:**546–563.
14. **Gunshin, H., B. Mackenzie, U. V. Berger, Y. Gunshin, M. F. Romero, W. F. Boron, S. Nussberger, J. L. Gollan, and M. A. Hediger.** 1997. Cloning and characterization of a mammalian proton-coupled metal-ion transporter. Nature **388:**482–488.
15. **Hantke, K.** 1987. Ferrous iron transport mutants in *Escherichia coli* K-12. FEMS Microbiol. Lett. **44:**53–57.
16. **Jabado, N., A. Jankowski, S. Dougaparsad, V. Picard, S. Grinstein, and P. Gros.** 2000. Natural resistance to intracellular infections. Natural resistance-associated macrophage protein 1 (NRAMP1) functions as a pH-dependent manganese transporter at the phagosomal membrane. J. Exp. Med. **192:**1237–1248.
17. **Janakiraman, A., and J. M. Slauch.** 2000. The putative iron transport system SitABCD encoded on SPI1 is required for full virulence of *Salmonella typhimurium*. Mol. Microbiol. **35:**1146–1155.
18. **Kawarabayasi, Y., Y. Hino, H. Horikawa, K. Jin-no, M. Takahashi, M. Sekine, S. Baba, A. Ankai, H. Kosugi, A. Hosoyama, S. Fukui, Y. Nagai, K. Nishijima, R. Otsuka, H. Nakazawa, M. Takamiya, Y. Kato, T. Yoshizawa, T. Tanaka, Y. Kudoh, J. Yamazaki, N. Kushida, A. Oguchi, K. Aoki, S. Masuda, M. Yanagii, M. Nishimura, A. Yamagishi, T. Oshima, and H. Kikuchi.** 2001.

Complete genome sequence of an aerobic thermoacidophilic crenarchaeon, *Sulfolobus tokodaii* strain 7. DNA Res. **8:**123–140.

19. **Kehres, D. G., M. L. Zaharik, B. B. Finlay, and M. E. Maguire.** 2000. The NRAMP proteins of *Salmonella typhimurium* and *Escherichia coli* are selective manganese transporters involved in the response to reactive oxygen. Mol. Microbiol. **36:**1085–1100.

19a. **Kehres, D. G., A. Janakiraman, J. M. Slauch, and M. E. Maguire.** 2002. Regulation of *Salmonella enterica* serovar Typhimurium *mntH* transcription by H_2O_2, Fe^{2+}, and Mn^{2+}. J. Bacteriol. **184:**3151–3158.

20. **Kimura, M., M. Ujihara, and K. Yokoi.** 1996. Tissue manganese levels and liver pyruvate carboxylase activity in magnesium-deficient rats. Biol. Trace Elem. Res. **52:**171–179.

21. **Kuhn, D. E., B. D. Baker, W. P. Lafuse, and B. S. Zwilling.** 1999. Differential iron transport into phagosomes isolated from the RAW264.7 macrophage cell lines transfected with Nramp1Gly169 or Nramp1Asp169. J. Leukoc. Biol. **66:**113–119.

22. **Lang, T., E. Prina, D. Sibthorpe, and J. M. Blackwell.** 1997. Nramp1 transfection transfers Ity/Lsh/Bcg-related pleiotropic effects on macrophage activation: influence on antigen processing and presentation. Infect. Immun. **65:**380–386.

23. **Liu, J., T. M. Fujiwara, N. T. Buu, F. O. Sanchez, M. Cellier, A. J. Paradis, D. Frappier, E. Skamene, P. Gros, and K. Morgan.** 1995. Identification of polymorphisms and sequence variants in the human homologue of the mouse natural resistance-associated macrophage protein gene. Am. J. Hum. Genet. **56:**845–853.

24. **Makui, H., E. Roig, S. T. Cole, J. D. Helmann, P. Gros, and M. F. Cellier.** 2000. Identification of the *Escherichia coli* K-12 NRAMP orthologue (MntH) as a selective divalent metal ion transporter. Mol. Microbiol. **35:**1065–1078.

25. **Que, Q., and J. D. Helmann.** 2000. Manganese homeostasis in *Bacillus subtilis* is regulated by MntR, a bifunctional regulator related to the diphtheria toxin repressor family of proteins. Mol. Microbiol. **35:**1454–1468.

26. **Rimon, A., Y. Gerchman, Y. Olami, S. Schuldiner, and E. Padan.** 1995. Replacements of histidine 226 of NhaA-Na^+/H^+ antiporter of *Escherichia coli*. Cysteine (H226C) or serine (H226S) retain both normal activity and pH sensitivity, aspartate (H226D) shifts the pH profile toward basic pH, and alanine (H226A) inactivates the carrier at all pH values. J. Biol. Chem. **270:**26813–26817.

27. **Sacher, A., A. Cohen, and N. Nelson.** 2001. Properties of the mammalian and yeast metal-ion transporters DCT1 and Smf1p expressed in *Xenopus laevis* oocytes. J. Exp. Biol. **204:**1053–1061.

28. **Scheuhammer, A. M., and M. G. Cherian.** 1983. The influence of manganese on the distribution of essential trace elements. II. The tissue distribution of manganese, magnesium, zinc, iron, and copper in rats after chronic manganese exposure. J. Toxicol. Environ. Health **12:**361–370.

29. **Silver, S., P. Johnseine, and K. King.** 1970. Manganese active transport in *Escherichia coli*. J. Bacteriol. **104:**1299–1306.

30. **Vidal, S. M., E. Pinner, P. Lepage, S. Gauthier, and P. Gros.** 1996. Natural resistance to intracellular infections: Nramp1 encodes a membrane phosphoglycoprotein absent in macrophages from susceptible (Nramp1 D169) mouse strains. J. Immunol. **157:**3559–3568.

31. **Zhou, D., W. D. Hardt, and J. E. Galan.** 1999. *Salmonella typhimurium* encodes a putative iron transport system within the centisome 63 pathogenicity island. Infect. Immun. **67:**1974–1981.